

# DIPHOTON PRODUCTION IN $pp$ COLLISION AT NLO: SIGNAL ANALYSIS\*

NADINE HAMMOUD

Institute of Nuclear Physics Polish Academy of Sciences, Kraków, Poland

(Received June 1, 2020)

We present the analysis of the SM Higgs boson main production channel,  $gg \rightarrow H$ , and the two photon Higgs decay channel  $H \rightarrow \gamma\gamma$  at tree level in order to obtain the differential cross section of  $gg \rightarrow H \rightarrow \gamma\gamma$  convoluted with the parton distribution functions (PDFs), and reproduce its plot as a function of the diphoton invariant mass distribution  $M_{\gamma\gamma}$ . Subsequently, we investigate the applicability of the heavy top-quark approximation in Singlet Higgs boson production and decay, and present a complete next-to-leading order calculation for  $gg \rightarrow H \rightarrow \gamma\gamma$ .

DOI:10.5506/APhysPolBSupp.14.195

## 1. Introduction

Although the way that SM describes what matter is made of and how it holds together is very simple, powerful and elegant, it fails to explain almost certainly genuine features of nature such as: gravity, baryon asymmetry, Dark Matter, *etc.* Hence, SM is an intermediate step towards a more fundamental theory, this is what motivates the particle physics society to search for physics beyond SM that can answer these unsolved questions. The motivation behind this work was the observation of the diphoton resonance with a mass of approximately 750 GeV at the LHC in the diphoton spectrum. There are at least 500 papers that can accommodate the observed diphoton signal — one can find a summary of the main models discussed in [1]. Thus, if this result was not simply a statistical fluctuation that disappeared with more data, it would have been an important implication not only for particle physics but also for cosmology.

---

\* This work was done under the supervision of Prof. Jean-Philippe Guillet at the Laboratory of Theoretical Physics — Annecy le Vieux, and presented at *Excited QCD 2020*, Krynica Zdrój, Poland, February 2–8, 2020.

### 2. Leading order calculations

In order to find the total differential cross section of the process  $gg \rightarrow H \rightarrow \gamma\gamma$  and to simplify our calculations, we divided this process into two subprocesses: Higgs production subprocess and Higgs decay subprocess.

#### 2.1. Higgs production: Gluon–gluon channel

The dominant Higgs production mechanism within the SM is the loop-induced gluon-fusion process  $gg \rightarrow H$  [2, 3]. In the SM, there is no direct coupling between gluons and Higgs particle, thus the LO contributions to this process is a one-loop Feynman diagram of intermediate quarks. The amplitude of the first diagram (left) of Fig. 1 reads

$$\begin{aligned}
 M_{ab}^{\mu\nu} &= g_s^2 \left(\frac{m_q}{v}\right) \mu^\varepsilon \text{Tr} \left[ T^a T^b \right] \epsilon_\mu^a(p_1) \epsilon_\nu^b(p_2) \\
 &\times \int \frac{d^n l}{(2\pi)^n} \text{Tr} \left[ \frac{\gamma^\mu (\not{l} + \not{p}_1 + m_q) (\not{l} - \not{p}_2 + m_q) \gamma^\nu (\not{l} + m_q)}{((l + p_1)^2 - m_q^2 + i\varepsilon)((l - p_2)^2 - m_q^2 + i\varepsilon)(l^2 - m^2 + i\varepsilon)} \right],
 \end{aligned}
 \tag{2.1}$$

where  $p_1$  and  $p_2$  are the four-momenta of the incoming gluons. We performed our calculation by applying the dimensional regularization technique [4, 5] to deal with the ultraviolet divergences due to the high-momentum limits of the loop integrals. After using Feynman parametrization:  $\frac{1}{ABC} = \int_0^1 dy \int_0^1 dx \frac{2}{(Axy + B(1-x)y + C(1-y))^3}$  and evaluating the loop integral numerator in the shifted loop momentum, one can define the transition amplitude as

$$\begin{aligned}
 M_{ab}^{\mu\nu} &= ig_s^2 \mu^\varepsilon \frac{4}{(4\pi)^2} \frac{m_q^2}{v} \frac{\delta_{ab}}{2} \left( g^{\mu\nu} - \frac{2p_1^\nu p_2^\mu}{M_H^2} \right) \frac{M_H^2}{2m_q^2} \\
 &\times \left[ 2 \frac{m_q^2}{M_H^2} + \left( 1 - 4 \frac{m_q^2}{M_H^2} J \left( \frac{m_q^2}{M_H^2} \right) \right) \right] \epsilon_a^\mu \epsilon_b^\nu \\
 &= g_s^2 \frac{i}{(4\pi)^2} \frac{gm_q^2}{M_w} \delta_{ab} \epsilon_a^\mu \epsilon_b^\nu \left( g^{\mu\nu} - \frac{2p_1^\nu p_2^\mu}{M_H^2} \right) \frac{M_H^2}{2m_q^2} \sum_q F(z),
 \end{aligned}
 \tag{2.2}$$

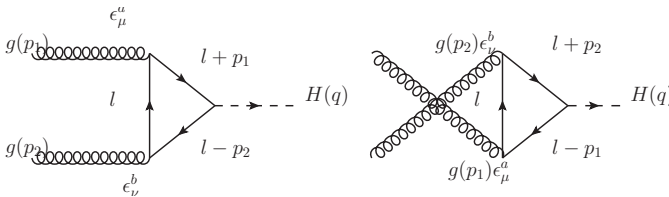


Fig. 1. The two contributing Feynman diagrams of  $gg \rightarrow H$  at tree level with the notation as used in the text.

with  $F(z) = 2z + (1 - 4z)J(z)$ , where  $J(z) = -\frac{z}{2} \log^2(1 - \frac{1}{x_1})$ , and  $z = \frac{m_q^2}{M_H^2}$ ,  $g = 2\frac{M_w}{v}$ , where  $M_w$ ,  $M_H$  are the  $W$  boson and Higgs boson masses respectively. The amplitude of the second diagram gives the exact same contributions as the first. Since all quarks except for the top quark will give almost negligible contributions to the diagram, we can define the effective vertex of the process  $gg \rightarrow H$  considering only a top-quark loop as

$$V_{ab}^{\mu\nu} = \frac{g}{2\pi} \frac{M_H^2}{M_w} \left( g^{\mu\nu} - \frac{2p_1^\nu p_2^\mu}{M_H^2} \right) \alpha_s \frac{i\delta_{ab}}{2} F \left( \frac{m_t^2}{M_H^2} \right), \quad \text{where } \alpha_s = \frac{g_s^2}{4\pi}. \quad (2.3)$$

## 2.2. Higgs decay: Diphoton channel

The decay into two photons channel is an important channel in the search for light Higgs boson at the LHC. In the SM, there is no direct coupling between Higgs and photons [6], hence this process proceeds through loops of intermediate gauge bosons ( $W$  bosons) and quarks (top quarks) [7].

### 2.2.1. Higgs boson decay into two photons via $W$ boson loop

The Feynman diagrams of this decay are shown in Fig. 2, and each one of them is highly divergent. To evaluate the total amplitude, we used the following expressions:

$$R_{\alpha\beta} = iv \frac{g^2}{2} g^{\alpha'\beta'} \left[ -i \frac{g_{\alpha\alpha'} - \frac{(k+q)_\alpha(k+q)_{\beta'}}{M_w^2}}{((k+q)^2 - M_w^2 + i\varepsilon)} \right] \left[ -i \left( \frac{g_{\beta\beta'} - \frac{k_\alpha k_\beta}{M_w^2}}{(k^2 - M_w^2 + i\varepsilon)} \right) \right], \quad (2.4)$$

$$\begin{aligned} M_1^{\mu\nu\alpha\beta} &= (ie) \left[ g^{\mu\beta}(-p_4 - k - q)^\delta + g^{\beta\delta}(2k + p_3 + q)^\mu + g^{\delta\mu}(-k - p_3 + p_4)^\beta \right] \\ &\times \left[ -i \left( g_{\delta\sigma} - \frac{(k + p_3)_\delta(k + p_3)_\sigma}{M_w^2} \right) \frac{1}{((k + p_3)^2 - M_w^2 + i\varepsilon)} \right] \\ &\times (ie) \left[ g^{\nu\sigma}(-2p_3 - k)^\alpha + g^{\sigma\alpha}(2k + p_3)^\nu + g^{\alpha\nu}(-k + p_3)^\sigma \right] \\ &\times \epsilon_\nu^*(p_3) \epsilon_\mu^*(p_4), \end{aligned} \quad (2.5)$$

$$M_2^{\mu\nu\alpha\beta} = M_1^{\mu\nu\alpha\beta} (\mu \leftrightarrow \nu, p_3 \leftrightarrow p_4), \quad (2.6)$$

$$M_3^{\mu\nu\alpha\beta} = (ie^2) \left[ g^{\alpha\nu} g^{\beta\mu} + g^{\alpha\mu} g^{\beta\nu} - 2g^{\alpha\beta} g^{\mu\nu} \right] \epsilon_\nu^*(p_3) \epsilon_\mu^*(p_4), \quad (2.7)$$

where  $R_{\alpha\beta}$  is the common part,  $M_i^{\mu\nu\alpha\beta}$  is their transition amplitude without  $R_{\alpha\beta}$ ,  $q$  is the Higgs boson momentum,  $p_3$  and  $p_4$  are the four-momenta of the outgoing photons. We used Feynman parametrization, dimensional regularization and a FORM code to evaluate the transition amplitudes of

each diagram. Finally, one can define the transition amplitude of  $H \rightarrow \gamma\gamma$  via  $W$  boson loop as

$$T = i \frac{M_H^2}{M_w} \frac{g}{2\pi} \alpha \left( g^{\mu\nu} - \frac{2p_3^\mu p_4^\nu}{M_H^2} \right) \frac{1}{2} G(z_w) \epsilon_\mu^*(p_4) \epsilon_\nu^*(p_3), \quad (2.8)$$

where  $G(z_w) = 1 + 6z_w + 6(1 - 2z_w)J(z_w)$ ,  $g = \frac{2M_w}{v}$  and  $\alpha = \frac{e^2}{4\pi}$ .

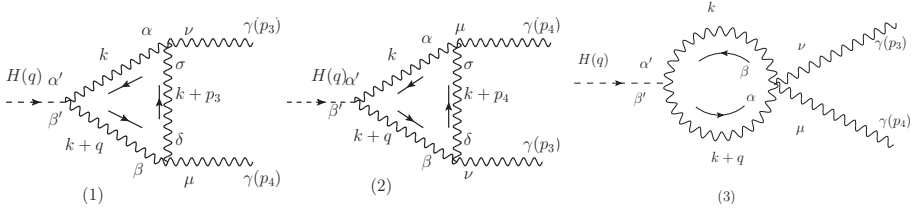


Fig. 2. Representative Feynman diagrams of the Higgs boson decay into two photons through  $W$  loop at tree level.

### 2.2.2. Higgs boson decay into two photons via Fermion loop

The Feynman diagrams of this process can be easily found from those of Higgs production with small modification where  $g \leftrightarrow \gamma$ . This process has also the exact same calculations as the Higgs production process.

By adding both contribution we define the  $H\gamma\gamma$  effective vertex as

$$V^{\mu\nu} = i \frac{g}{2\pi} \frac{M_H^2}{M_w} \left( g^{\mu\nu} - \frac{2p_4^\nu p_3^\mu}{M_H^2} \right) \times \alpha \left[ N_c \sum_q Q_q^2 F \left( \frac{m_q^2}{M_H^2} \right) + \sum_l Q_l^2 F \left( \frac{m_l^2}{M_H^2} \right) + \frac{1}{2} G \left( \frac{m_w^2}{M_H^2} \right) \right], \quad (2.9)$$

where  $N_c$  is the number of the quark's color,  $Q_l$  and  $Q_q$  are the electric charges of the lepton and quark respectively.

## 3. Differential cross section

In our current work, we are interested in calculating the total hadronic differential cross section defined as

$$d\sigma_{\text{had}} = \int dx_a \int dx_b f(x_a) f(x_b) d\hat{\sigma}_{\text{part}}, \quad (3.1)$$

where  $x_a$  and  $x_b$  are the longitudinal momentum fractions of each proton that is carried by the incoming gluons,  $f(x_{a,b})$  is the parton distribution function,

and  $d\hat{\sigma}_{\text{part}}$  is the partonic differential cross section. By using the hadronic center-of-mass frame kinematics, we showed that the hadronic differential cross section is

$$\frac{d\sigma}{dM_{\gamma\gamma}^2} = \frac{s^2}{128\pi^3(N_c^2-1)} \frac{\alpha^4\alpha_s^2}{\sin^4(\theta_w)} \frac{|Z|^2}{M_w^4} \left[ \sum_{a,b} \int dy_3 du_1 f_{g_a}(x_a, M^2) f_{g_b}(x_b, M^2) \right. \\ \left. \times \frac{1}{(x_a^2 e^{-2y_3} + x_b^2 e^{2y_3} + 2\tau)} x_a \frac{\tau^4}{((\tau s - M_H^2)^2 + \Gamma_H^2 M_H^2)^2} \right], \quad (3.2)$$

where  $Z = (\tau s - M_H^2 - i\Gamma_H M_H) \sum_q F(z_q) (2N_c \sum_q Q_q^2 F(z_q) + 2 \sum_l Q_l^2 F(z_l) + G(z_w))$ . To calculate this cross section we used a FORTRAN code with the LHAPDF library, then one can plot the invariant mass distribution of  $gg \rightarrow H \rightarrow \gamma\gamma$  at the center-of-mass energy of 8 and 13 TeV using Root.

## 4. Next to Leading Order calculations

To simplify our NLO calculations, we integrate out the top-quark loop into an effective vertex using the infinite top-quark mass approximation. The NLO calculations can be divided into two categories: virtual and real contributions. Each contribution is separately divergent, hence only the combination of the two components leads to a finite result.

### 4.1. Virtual contributions

There is no momentum or energy exchange between the initial and the final state of our process, so we can work on each subprocess separately

#### 4.1.1. Higgs production subprocess

The non-zero Feynman diagrams that give virtual contributions to  $gg \rightarrow H$  subprocess in the infinite top-quark mass limit are two: the vertex correction and the bubble with 4 gluon vertex diagrams as shown in Fig. 3. The virtual contributions to the cross section can be calculated using:  $d\hat{\sigma}_{\text{virt}} = d\text{PS} \sum 2\Re(M_{\text{virt}} M_0^*)$ , where  $d\text{PS}$  is the one particle phase space and  $(M_0^*)$  is the complex conjugate of the leading order matrix element using the EFT. Virtual corrections to Higgs production arise from the interference between the Born and the one-loop amplitudes of the diagrams in Fig. 3, so to calculate these interference terms we employed a FORM code. While calculating these terms, one will encounter an infrared and ultraviolet divergences, so applying dimensional regularization techniques is recommended. In addition, we should take into account the virtual contributions of the

hidden top-quark loop that can be parametrized as:  $M_Q = M_Q^{\text{LO}}(1 + \frac{\alpha_s}{\pi} \frac{11}{4})$  [8]. Thus, the final expression of the virtual cross section is

$$d\sigma_{\text{virt}} = \frac{1}{1-\varepsilon} \frac{\alpha_s^2}{v^2} \frac{s^2}{36\pi^2(N_c^2 - 1)} \frac{\alpha_s}{2\pi} \left( \frac{4\pi\mu^2}{Q^2} \right)^\varepsilon d\phi_2 r_\Gamma \times \left[ \frac{-N_c}{\varepsilon^2} + \frac{N_c}{\varepsilon} \log\left(\frac{s^2}{Q^2}\right) - \frac{1}{\varepsilon} b_{gg} \delta(1-z) + \frac{N_c\pi^2}{2} \right], \quad (4.1)$$

where  $r_\Gamma = \frac{\Gamma(1+\varepsilon)\Gamma^2(1-\varepsilon)}{\Gamma(1-2\varepsilon)}$ ,  $b_{gg} = \frac{11N_c - 2N_f}{6}$  with  $N_f$  being the number of the light quarks.

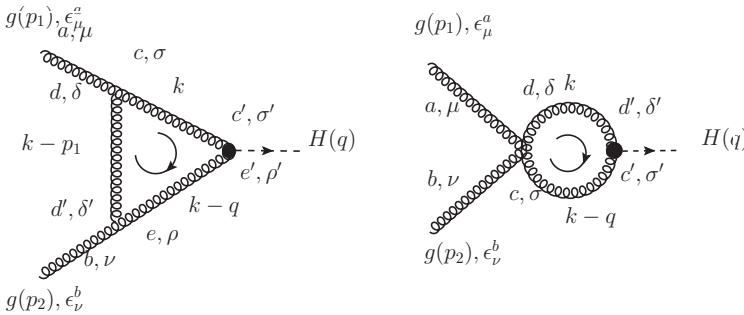


Fig. 3. Feynman diagrams giving virtual contributions to the subprocess  $gg \rightarrow H$  at infinite top-quark mass limit, note that the dot represents the effective  $Hgg$  vertex.

#### 4.1.2. Higgs decay subprocess

The radiative corrections to this subprocess affect only the top-quark loop and neither the  $W$  loop nor the final-state photons, hence according to Ref. [9], the QCD correction factor of the quark contribution to the  $H\gamma\gamma$  coupling in the infinite top-quark mass limit is  $1 - \frac{\alpha_s}{\pi}$ . Therefore, the virtual cross section of the Higgs decay subprocess can be written as

$$d\sigma_{H \rightarrow \gamma\gamma} = \frac{1}{64\pi(1-\varepsilon)} \frac{\alpha^2}{v^2} z\delta(1-z)|A|^2 \left[ 1 - \frac{\alpha_s}{\pi} \right], \quad \text{where } z = \frac{M_H^2}{\hat{s}}. \quad (4.2)$$

#### 4.2. Real contributions

The real contribution to  $gg \rightarrow gH$  is found from the Feynman diagrams of Fig. 4. We first computed the  $Hggg$  vertex using the effective Lagrangian to

find the matrix element of each diagram. Then, by employing a FORM code, one can easily find the averaged total matrix element squared of  $gg \rightarrow gH$

$$\overline{|M(gg \rightarrow H)|^2} = \frac{\alpha_s^3}{24\pi v^2} \frac{1}{(1 - \varepsilon)^2} \times \left[ \left( \frac{M_H^8 + s^2 + u^4 + t^4}{stu} \right) (1 - 2\varepsilon) + \frac{\varepsilon}{2} \left( \frac{(M_H^4 + s^2 + t^2 + u^2)^2}{stu} \right) \right]. \quad (4.3)$$

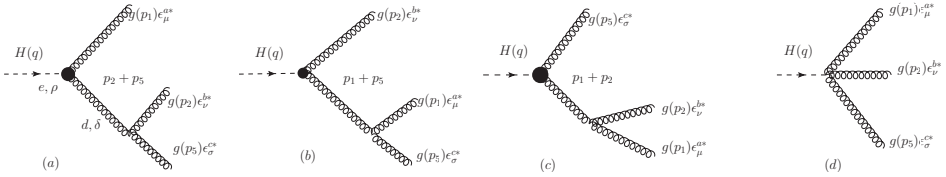


Fig. 4. Representative Feynman diagrams to the subprocess  $gg \rightarrow gH$ .

### 4.3. Hard and soft physics talking

After calculating both virtual and real contributions to  $gg \rightarrow H$ , we see that these contributions are not IR safe, *e.g.* in the real contributions,  $p_5$  (the emitted real gluon momentum) can be soft or collinear to another momentum. Then, we regulated and isolated these singularities so that in intermediate stages the singularities appear as single and double poles in  $\varepsilon$ . Unlike the virtual corrections, the divergences contained in the real corrections are implicitly hidden in the phase-space integration. Let  $\xi = 2E_5/\sqrt{s}$  be the reduced energy, and  $\xi_c$  be the cutoff parameter to separate the gluon phase space to soft and hard regions. The soft regions contain both soft and collinear divergences, while the hard regions contain only collinear singularities. Hence, the emitted gluon energy in the soft regions satisfies:  $E_5 \leq \xi_c \frac{\sqrt{s}}{2}$ , while for the hard regions, we have  $E_5 \geq \xi_c \frac{\sqrt{s}}{2}$ . In order to get the finite part, we used FKS method [10, 11]. Hereby, after adding both virtual and soft term of real contributions, all the IR divergences will cancel out and we will end up with two collinear divergences. Then, by adding our result to the collinear terms of the real contribution and taking limits of  $z = 1$ , all the collinear divergences from soft part will cancel and the remaining ones will be factorized and absorbed in the PDFs. In order to compute a complete NLO cross section, one should take into account the extra partonic channels that appeared, namely the  $gq \rightarrow qH$  and  $q\bar{q} \rightarrow gH$ , Ref. [8] and to study their corrections. At the end and after adding all the resultant finite terms and employing a well-developed FORTRAN code, one can calculate the total NLO cross section of  $gg \rightarrow H \rightarrow \gamma\gamma$ .

## 5. Conclusion

At least next-to-leading order perturbative calculations are required for most LHC processes analyses, since they provide us with an accurate QCD predictions and reliable error estimates. Furthermore, the extra partonic channels appearing at NLO can have a significant impact on differential distributions. Moreover, one can observe that using effective field theory at NLO simplifies the calculations and reduces the scale uncertainties. Finally, the presented method can be used for any new scalar resonance that may appear in the diphoton channel. This paper presents an ongoing work to build a flexible program describing the exchanges of exotic particles between the  $gg$  initial state and the  $\gamma\gamma$  final one.

The author would like to thank Prof. Jean-Philippe Guillet for his useful advice, guidance and support, and the organizers of the *Excited QCD 2020* conference for the very pleasant workshop. This work has been partially supported by the National Science Center, Poland (NCN) grant No. 2018/29/B/ST2/02576.

## REFERENCES

- [1] A. Strumia, [arXiv:1605.09401 \[hep-ph\]](#).
- [2] H.M. Georgi, S.L. Glashow, M.E. Machacek, D.V. Nanopoulos, *Phys. Rev. Lett.* **40**, 692 (1978).
- [3] J. Gunion, H. Haber, G. Kane, S. Dawson, «The Higgs Hunter's Guide», Addison–Wesley, Reading, Mass. 1990.
- [4] G. Serman, «An Introduction to Quantum Field Theory», *Cambridge University Press*, 1993.
- [5] M.E. Peskin, D.V. Schroeder, «An Introduction to Quantum Field Theory», Westview Press, 1995.
- [6] S.L. Glashow, *Nucl. Phys.* **22**, 579 (1961); S. Weinberg, *Phys. Rev. Lett.* **19**, 1264 (1967); A. Salam, in: N. Svartholm (Ed.) «Elementary Particle Physics: Relativistic Groups and Analyticity. Eighth Nobel Symposium», *Almqvist and Wiksell*, Stockholm 1968, p. 367.
- [7] F. Bursa *et al.*, *Phys. Rev. D* **85**, 093009 (2012), [arXiv:1112.2135 \[hep-ph\]](#).
- [8] S. Dawson, *Nucl. Phys. B* **359**, 283 (1991).
- [9] M. Spira, A. Djouadi, D. Graudenz, P.M. Zerwas, *Nucl. Phys. B* **453**, 17 (1995), [arXiv:hep-ph/9504378](#).
- [10] S. Frixione, *Nucl. Phys. B* **507**, 295 (1997), [arXiv:hep-ph/9706545](#).
- [11] S. Frixione, Z. Kunszt, A. Signer, *Nucl. Phys. B* **467**, 399 (1996), [arXiv:hep-ph/9512328](#).